

# Radially truncated galactic discs<sup>☆</sup>

Richard de Grijs<sup>1,2,†</sup>, Michiel Kregel<sup>3</sup> and Karen H. Wesson<sup>1,‡</sup>

<sup>1</sup> *Astronomy Department, University of Virginia, PO Box 3818, Charlottesville, VA 22903, USA*

<sup>2</sup> *Institute of Astronomy, University of Cambridge, Madingley Road, Cambridge CB3 0HA*

<sup>3</sup> *Kapteyn Astronomical Institute, University of Groningen, PO Box 800, 9700 AV Groningen, the Netherlands*

Received date; accepted date

## ABSTRACT

We present the first results of a systematic analysis of radially truncated exponential discs for four galaxies of a complete sample of disc-dominated edge-on spiral galaxies. The discs of our sample galaxies are truncated at similar radii on either side of their centres. With possible the exception of the disc of ESO 416-G25, it appears that the truncations in our sample galaxies are closely symmetric, in terms of both their sharpness and the truncation length. However, the truncations occur over a larger region and not as abruptly as found in previous studies.

We show that the truncated luminosity distributions of our sample galaxies, if also present in the mass distributions, comfortably meet the requirements for longevity. The formation and maintenance of disc truncations are likely closely related to stability requirements for galactic discs.

**Key words:** galaxies: formation – galaxies: fundamental parameters – galaxies: photometry – galaxies: spiral – galaxies: structure

## 1 INTRODUCTION

It is well-known from Freeman's (1970) work that the radial light distribution of the stellar component of high surface brightness galactic discs can be approximated by an exponential law of the form

$$L(R) = L_0 \exp(-R/h_R) \quad (1)$$

where  $L_0$  is the luminosity density in the galactic centre,  $R$  the galactocentric distance and  $h_R$  the disc scalelength.

However, for a few prominent high surface-brightness edge-on galaxies, it has initially been shown by van der Kruit & Searle (1981a,b, 1982a,b, hereinafter KS1–4), that at some radius  $R_{\max}$  (the truncation or cut-off radius of the galactic disc) the stellar luminosity distribution disappears asymptotically into the background noise (see also Jensen & Thuan 1982, Sasaki 1987, Morrison, Boroson & Harding 1994, Bottema 1995, Lequeux, Dantel-Fort & Fort 1995, Näslund & Jörsäter 1997, Fry et al. 1999, Pohlen et al. 2000a,b). In fact, the truncation of galactic discs does not occur instantly but over a small region, where the luminosity decrease becomes much steeper, having exponential scalelengths of order or

less than a kiloparsec, opposed to several kpc in the exponential disc part (e.g., KS1–4, Jensen & Thuan 1982, Sasaki 1987, Abe et al. 1999, Fry et al. 1999).

An independent approach to obtain the statistics of truncated galactic discs, using a sample of galaxies selected in a uniform way, is needed in order to better understand the overall properties and physical implications of this feature. In this paper we present the first results of a systematic analysis of disc truncations for a pilot sample of four “normal” spiral galaxies, drawn from the statistically complete sample of edge-on disc-dominated galaxies of de Grijs (1998). In Kregel, van der Kruit & de Grijs (2001) we will present a re-analysis of the global disc structures of the entire de Grijs (1998) sample, including a systematic analysis of the occurrence of truncated galactic discs.

Edge-on galaxies are particularly useful for the study of truncated galactic discs: since these disc cut-offs usually occur at very low surface brightness levels, they are more readily detected in highly inclined galaxies, where we can follow the light distributions out to larger radii. In Sect. 2 we outline the sample selection and our approach and methodology.

A detailed error discussion for our pilot sample is given in Sect. 3. The most important science driver for the study of truncated galactic discs, discussed in Sect. 4, is that if the truncations seen in the stellar light are also present in the mass distribution, they would have important dynamical consequences at the disc's outer edges.

<sup>☆</sup> Based on observations obtained at the European Southern Observatory, La Silla, Chile

<sup>†</sup> E-mail: grijs@ast.cam.ac.uk

<sup>‡</sup> Present address: Center for Hydrologic Science, Duke University, 106 Old Chemistry, Box 90230, Durham, NC 27708, USA

## 2 GLOBAL APPROACH

### 2.1 Pilot sample

We selected four galaxies from the statistically complete sample of disc-dominated edge-on galaxies of de Grijs (1998) for this pilot study.

The galaxies in the parent sample were selected to:

- have inclinations  $i \geq 87^\circ$ ;
- have blue angular diameters  $D_{25}^B \geq 2.^{\prime}2$ ; and
- be non-interacting and undisturbed S0 – Sd galaxies.

We required these pilot galaxies to have relatively high signal-to-noise (S/N) ratios out to large galactocentric distances, thus allowing us to better determine the occurrence of a possible truncated disc at large radii. Of the parent sample of 48 edge-on disc galaxies,  $\sim 25$  met our overall high-S/N selection criteria in *all* of the  $B$ ,  $V$  and  $I$  observations. The four galaxies selected for our pilot sample were chosen randomly from among the larger disc galaxies because of their small bulge-to-disc ratio and well-defined, regular disc component, which was only negligibly or minimally affected by a central dust lane (cf. Fig. 2 in Chapter 9 of de Grijs 1997).

The basic physical properties of these pilot sample galaxies are summarised in Table 1. The observational properties were taken from de Grijs (1997, 1998). The derived properties are obtained in Sect. 2.3.1. They are based on the detailed modelling of the galactic luminosity density distributions projected on the plane of the sky using the method described in Kregel et al. (2001). The detailed observational logs of and data reduction techniques applied to our  $B$ ,  $V$  and  $I$ -band observations are summarised in de Grijs (1998). Fig. 1 displays the  $I$ -band contours of these galaxies.

### 2.2 The adopted three-dimensional model

We will approximate the three-dimensional (3D) luminosity density of the discs of “ideal” spiral galaxies as a combination of independent exponential light distributions in both the radial and the vertical directions (see, e.g., de Grijs, Peletier & van der Kruit [1997] for a statistical approach to determine the latter behaviour), for all radii excluding the region of truncation. In view of the finite extent of the cut-off region,  $\delta$ , and to avoid discontinuities in the luminosity and density distributions, we will adopt a slightly modified version of Casertano’s (1983) mathematically convenient description for a “soft cut-off” of the radial density distribution in the truncation region. His model assumes that in the region beyond  $(R_{\max} - \delta)$ , the radial luminosity density decreases linearly to zero:

$$L(R) = L_0 \begin{cases} \exp(-R/h_R), & \text{if } R \leq (R_{\max} - \delta) \\ \exp\left(-\left(\frac{R_{\max} - \delta}{h_R}\right)\left[\frac{1 - \left(\frac{R - (R_{\max} - \delta)}{\delta}\right)}{\delta}\right]\right), & \text{if } (R_{\max} - \delta) \leq R \leq R_{\max} \\ 0, & \text{if } R > R_{\max}. \end{cases} \quad (2)$$

A model radial profile with a “soft cut-off” will therefore show an exponentially declining disc component, displaying an abrupt steepening at the onset of the truncation region at  $(R_{\max} - \delta)$ , decreasing linearly until the background noise

level is reached. We will use a slightly modified version of Eq. (2), in which the radial luminosity density decreases exponentially instead of linearly until it disappears into the background noise. Examples of our modified fitting function are shown in Fig. 6 for the current sample.

The exact functional form of the radial luminosity density in the cut-off region is unknown because of the limited spatial resolution and low S/N ratio at these large galactocentric distances. Thus, within the observational uncertainties, Casertano’s (1983) description of the “soft cut-off” does not deviate significantly from this simple exponential form, also adopted by Jensen & Thuau (1982) and Näsland & Jörsäter (1997) to fit the truncated light profiles of NGC 4565. Furthermore, our approach, using the exponentially decreasing radial functionality in the truncation region, will provide us with an additional constraint on the shape of the truncation region compared to Casertano’s (1983), namely the scale length in the truncation region,  $h_{R,\delta}$ .

In the case of an edge-on orientation, the projection onto the plane of the sky of our model radial exponential luminosity density distribution is, for  $R \leq (R_{\max} - \delta)$ , closely approximated by (KS1):

$$L(R) = L_0 \frac{R}{h_R} K_1\left(\frac{R}{h_R}\right), \quad (3)$$

where  $K_1$  is the modified Bessel function of the first order.

The total projected 3D luminosity density is now given by

$$L(R, z) = L(R) \exp(-z/h_z) , \quad (4)$$

where  $z$  is the (vertical) distance from the galactic plane and  $h_z$  the exponential scaleheight.

#### 2.2.1 Differences with respect to earlier work

Except for a few detailed studies of individual large edge-on galaxies (e.g., KS1, Jensen & Thuau 1981, Sasaki 1987, Näsland & Jörsäter 1997, Abe et al. 1999, Fry et al. 1999), most previous analyses aimed at determining disc truncations for statistically more meaningful samples (e.g., KS3, Barteldrees & Dettmar 1994, Pohlen et al. 2000a,b) have adopted a number of *a priori* assumptions that may not be fully justified. In particular, these studies assumed that:

- (i) galactic discs are truncated at equal radii on either side of the galactic centre, and
- (ii) the radial surface brightness distributions disappear asymptotically (“vertically”) into the background noise at  $R_{\max}$ .

While the first assumption may approximate the observational situation relatively closely (cf. Sect. 3.3.2 for the current pilot sample), the surface brightness generally does not disappear asymptotically into the noise for most of the well-resolved galaxies studied to date.

Forcing a fitting routine to satisfy both of these assumptions in galaxies with slightly different truncation radii on either side of the centre will often overpredict the surface brightness in one of the truncation regions significantly (depending on the extent of this region), even if the full projected 3D surface brightness distribution is used. This is clearly illustrated in Pohlen et al. (2000b), in particular in their  $i$ -band fits to the brightest profiles parallel to the major

**Table 1.** Basic properties of the pilot sample galaxies

Columns: (1) Galaxy name (Lauberts & Valentijn 1989; ESO-LV); (2) and (3) Coordinates; (4) Revised Hubble Type; (5) Blue major axis diameter,  $D_{25}^B$ ; (6) Passband observed in; (7) apparent magnitude, corrected for foreground extinction; (8) extrapolated edge-on disc central surface brightness; (9) Exponential scaleheight; (10) Exponential scalelength.

Galaxy	RA (J2000)	Dec	Type	$D_{25}^B$	Passband	$m_0$	$\mu_0$	$h_z$	$h_R$
(1)	(2)	(3)	(4)	(5)	(6)	(mag)	(mag arcsec $^{-2}$ )	(")	(")
						(7)	(8)	(9)	(10)
ESO 201-G22	04 08 59.3	-48 43 42	5.0	2.52	<i>B</i>	$14.06 \pm 0.07$	$20.54 \pm 0.07$	$2.4 \pm 0.1$	$26.9 \pm 1.5$
					<i>V</i>		$20.39 \pm 0.10$	$2.4 \pm 0.1$	$25.2 \pm 1.1$
					<i>I</i>	$13.10 \pm 0.03$	$19.23 \pm 0.08$	$2.6 \pm 0.2$	$23.3 \pm 1.3$
ESO 416-G25	02 48 40.8	-31 32 07	3.0	2.35	<i>B</i>	$14.42 \pm 0.11$	$21.41 \pm 0.03$	$3.1 \pm 0.1$	$29.2 \pm 1.4$
					<i>V</i>		$20.90 \pm 0.08$	$3.5 \pm 0.2$	$25.8 \pm 1.3$
					<i>I</i>	$12.52 \pm 0.03$	$19.87 \pm 0.05$	$3.6 \pm 0.2$	$22.2 \pm 2.0$
ESO 446-G18	14 08 37.9	-29 34 20	3.0	2.52	<i>B</i>	$15.12 \pm 0.05$	$20.72 \pm 0.10$	$2.2 \pm 0.1$	$22.5 \pm 1.3$
					<i>V</i>		$20.03 \pm 0.08$	$2.2 \pm 0.1$	$19.5 \pm 0.9$
					<i>I</i>	$12.71 \pm 0.02$	$18.49 \pm 0.10$	$2.0 \pm 0.2$	$18.1 \pm 1.4$
ESO 446-G44 (= IC 4393)	14 17 49.3	-31 20 55	6.0	2.67	<i>B</i>	$14.83 \pm 0.03$	$20.39 \pm 0.10$	$2.1 \pm 0.1$	$25.1 \pm 0.7$
					<i>V</i>		$19.76 \pm 0.07$	$2.0 \pm 0.1$	$24.5 \pm 0.6$
					<i>I</i>	$12.51 \pm 0.04$	$18.90 \pm 0.15$	$2.7 \pm 0.2$	$29.5 \pm 1.6$

axis of the galaxies IC2207, IC4393, ESO446-G18, ESO466-G01 and ESO578-G25. Alternatively, if the truncation radii on either side of the centre are similar but the truncation scalelength is relatively long, forcing a 3D fitting routine to adopt sharp cut-offs as in the latter assumption, will *under* predict the actual radius where the galactic luminosity density disappears into the noise.

In view of these considerations, we will avoid such *a priori* assumptions in our approach; we will determine the actual truncation radii independently on either side of the galactic centre, and approximate the luminosity density distribution in the truncation region by an exponentially decreasing function of radius.

Examples of the fitting method for our pilot sample are presented in Sect. 3.3.

### 2.3 Surface brightness modelling

Although the determination of the actual truncation radius  $R_{\max}$  is relatively model-independent, for the detailed modelling of the truncation region ( $R_{\max} - \delta$ ), it is crucially important to determine accurate scale parameters (in particular scale lengths) for the main, exponential disc component, cf. Eqs. (2) and (3).

The surface brightness distributions of spiral galaxies often show significant local deviations from the assumed smooth, large-scale model distribution (3) (e.g., Seiden, Schulman & Elmegreen 1984, Shaw & Gilmore 1990, de Jong 1995, and references therein). This makes the global applicability of radial disc scalelengths obtained from radial profiles parallel to the major axes of edge-on galaxies very uncertain (e.g., Knapen & van der Kruit 1991, Giovanelli et al. 1994).

Therefore, we will model the global disc structures using the full projected luminosity density distributions of the galactic discs in our sample, using Eqs. (3) and (4), in the linear regime. An elaborate description of the method, as well as extensive tests on artificial images, will be presented in Kregel et al. (2001). This paper will only address the occurrence of disc truncations in the de Grijs (1998) sample,

without embarking on a detailed analysis of their shapes, however.

A number of potential problems are foreseen regarding the applicability of our simple model, Eq. (4), to the observed luminosity distributions of edge-on galaxies.

First, it does not include a description of the truncation region. A physically motivated, or even an empirical description of this region is, at this point, too premature and therefore this region will be masked out before least-squares minimization.

Secondly, the regions near the galactic planes are affected by extinction. Whilst these effects can be included by using a 3D radiative transfer code (e.g., Kylafis & Bahcall 1987, Xilouris et al. 1997), we choose to mask the data in the regions near the planes instead.

Thirdly, by adopting our simple model, Eq. (4), we do not include the effects of a truncated galactic disc along the line of sight. However, the effects of neglecting a line-of-sight truncation are small (see Kregel et al. 2001): while it may cause us to underestimate the disc scalelength of ESO446-G44 by  $\sim 15\%$ , the effect is  $\leq 8\%$  for the other galaxies in our sample, and is in practice counteracted by residual extinction by dust, if any, at the  $z$ -heights used in our study. In addition, this effect is negligible for the accurate determination of the disc *truncations* as such, the main aim of our study.

Before applying our fitting routine to the full observed luminosity density distributions, the sky-subtracted images needed to be prepared. First, foreground stars and background galaxies were masked out. Secondly, profiles parallel to the minor axis were taken at various distances along the major axis. These were subsequently inspected for extinction effects, leading to the masking out of the regions described below for the individual galaxies.

#### 2.3.1 Fits to the individual galaxies

We will now discuss the fits to the luminosity density of each galaxy individually, thereby addressing a number of prob-

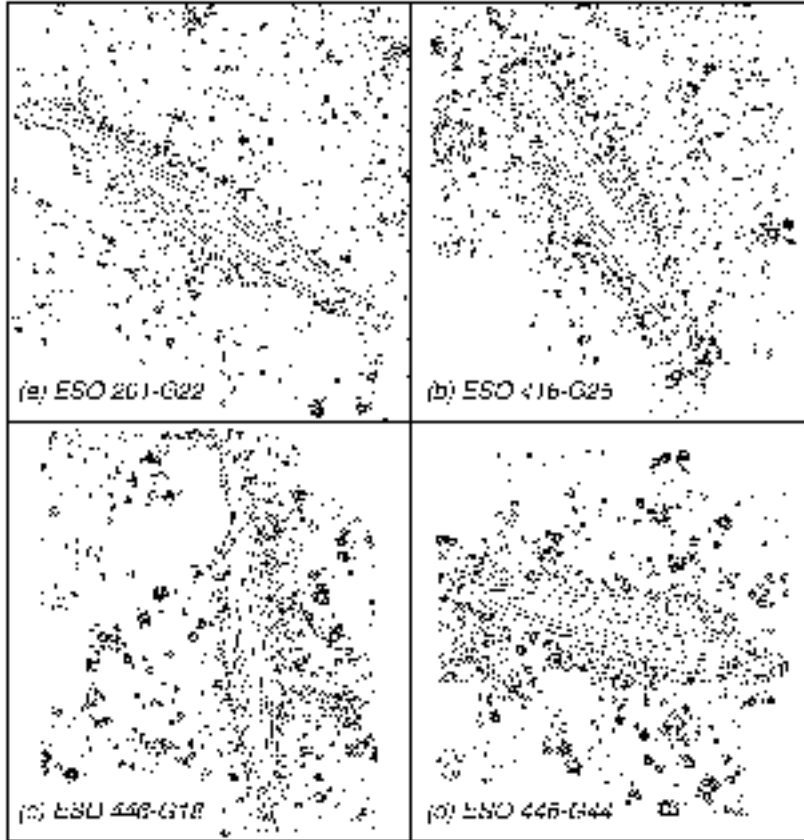


**Figure 1.** Optical  $I$ -band isophotes of the four edge-on disc galaxies in our pilot sample. North is up, East to the left; each panel is approx.  $3'$  on a side. The contours are spaced by 1.0 mag, starting from the lowest contours at  $23.5 \text{ } I\text{-mag arcsec}^{-2}$ . For reasons of clarity, the brightest foreground stars (that may be potentially contaminating the galactic discs) have been masked out. Note that an indication of the presence of disc truncations is already given by the rounded contours at the discs' outer edges.

lems encountered in each case. In all fits the galactic centres were fixed at the values determined by fitting ellipses to the  $I$ -band isophotes, using a custom-written IRAF<sup>§</sup> package for galactic surface photometry (“GALPHOT”).

In each case, conservative estimates of the onset of the truncation region and of the region near the galactic plane most affected by extinction were made based on detailed visual examinations of the radial and vertical luminosity distributions, respectively. The inner boundaries used for the radial fitting were chosen to minimize possible bulge effects and will be discussed individually below. Table 2 summa-

rizes the radial ranges adopted for the disc fits, as well as the vertical ranges excluded to avoid extinction effects.

Fig. 2 shows the  $I$ -band images and residual emission (disc model subtracted from the observations) for ESO 201-G22 and ESO 416-G25. Table 1 contains the resulting global scale parameters. The associated uncertainties are the observational errors, estimated by comparing results from several similar fits in which we adjusted the boundaries of the radial fitting range by 10–20%; the formal errors were in general less than 1%.

*ESO 201-G22* – Figs. 2a and b clearly show the bulge component and, just outside the masked region, the effects of either residual extinction near the galactic plane or, more likely, an additional disc component. The residuals in the fitted region do not show large systematic effects; the bulge contribution to the disc-dominated fitting range is negligible. The negative residuals extending to the edges of these fig-

<sup>§</sup> The Image Reduction and Analysis Facility (IRAF) is distributed by the National Optical Astronomy Observatories, which is operated by the Association of Universities for Research in Astronomy, Inc., under cooperative agreement with the National Science Foundation.

**Table 2.** Fitting regions

Columns: (1) Galaxy name; (2) and (3) Radial fitting range (arcsec); (4) and (5) Vertical region around the galactic plane excluded from the fits ( $h_z$ ).

Galaxy	Radial fitting		Galactic plane	
	$r_{\min}$ (1)	$r_{\max}$ (2)	$z_{\min}$ (4)	$z_{\max}$ (5)
ESO 201-G22	15	50	-1.0 (S)	1.0 (N)
ESO 416-G25	25	50	-1.0 (E)	1.0 (W)
ESO 446-G18	18	55	-2.0 (E)	0.5 (W)
ESO 446-G44	0	36	-1.5 (S)	1.5 (N)

ures clearly show the presence of a truncation in the galactic light distribution.

*ESO 416-G25* – This is the earliest-type galaxy in our pilot sample. The residuals after subtracting the disc-only fit (Fig. 2d) do not appear to be systematic in the region where the fit was done, and their amplitude is small (r.m.s. residual  $\approx 1.7 \sigma_{\text{background}}$ ). Although we included a bulge component, the 6-parameter fit proved to be very unstable.

*ESO 446-G18* – Figs. 1c and 4 show that this galaxy is not exactly edge-on. Extinction predominantly affects the eastern side. A dust mask placed symmetrically with respect to the major axis is therefore not appropriate. The residuals are relatively large (r.m.s. residual  $\approx 3.3 \sigma_{\text{background}}$ ) but do not appear to be systematic in the region where the fit was done. A fit including an exponential bulge did not converge.

*ESO 446-G44* – Surface brightness profiles of ESO 446-G44 do not reveal any bulge component. They do show, however, that ESO 446-G44 may not be exactly edge-on. Again, the residuals in the region where we applied our fitting routine are large (r.m.s. residual  $\approx 5.3 \sigma_{\text{background}}$ ) but do not appear to be systematic.

Having just obtained reliable global scale parameters for our sample galaxies, we are now ready to quantify the disc truncations occurring in these galaxies.

### 3 TRUNCATED DISCS

#### 3.1 Approach

In the analysis of edge-on galaxies, the inner disc region closest to the plane often needs to be avoided because of the presence of either a prominent dust lane, or a patchy dust distribution with its highest density towards the galactic plane. In many cases, the dust component extends all the way to the edge of the disc, thus making the luminosity distribution near the galactic planes useless for our study.

The exponential scaleheight of galactic discs is – to first order – constant as a function of galactocentric distance, at least for later-type disc galaxies (see, e.g., KS1–4, Kylafis & Bahcall 1987, Shaw & Gilmore 1990, Barnaby & Thronson 1992, de Grijs & Peletier 1997). Therefore, the radial luminosity distributions parallel to the galactic planes show a similar functional behaviour as the luminosity profiles *in* the plane in the absence of the dust component. Consequently, by extracting light profiles parallel to the galactic planes, we will also be able to study the occurrence and properties of radially truncated discs, provided that the S/N ratio allows us to detect such a truncation.

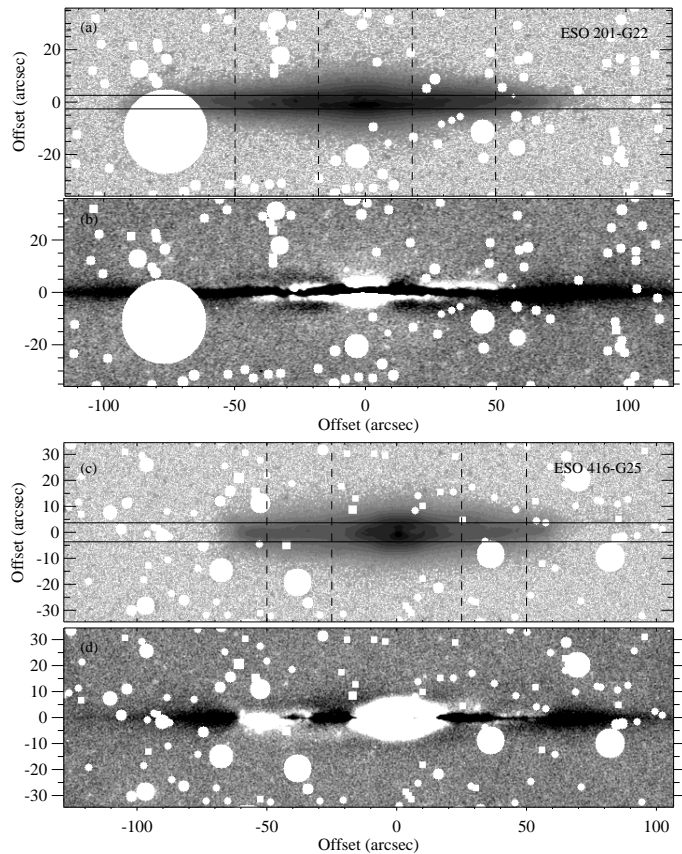


**Figure 2.** (a) – Negative  $I$ -band image of ESO 201-G22, after removal of foreground stars and background galaxies. The radial fitting boundaries are indicated by the dashed lines; the dust mask covering the region close to the plane affected by extinction is bracketed by the solid lines; (b) – Residuals for ESO 201-G22 after subtracting the model, greyscale levels range from  $-6\sigma_{\text{background}}$  (black) to  $+6\sigma_{\text{background}}$  (white) (c) and (d) – ESO 416-G25, as (a) and (b)

To find the optimum balance between avoiding contamination by the in-plane dust component on the one hand, and retaining a sufficiently high S/N ratio at large galactocentric distances on the other, numerous experiments were performed. In Fig. 3 we show ESO 416-G25 as an example, where we compare several radial profiles obtained on either side of the galactic plane. The solid lines in both panels represent the total profiles, vertically averaged over the entire half of the galactic disc (effectively for  $|z| \leq 8h_z$ ). They are obviously significantly affected by patchy dust and/or low S/N regions throughout the disc and are therefore discarded from further use. From this figure (and similar figures for the other galaxies in our sample) it follows that either the range  $(1.0 \leq |z| \leq 2.0h_z)$  or  $(1.5 \leq |z| \leq 3.5h_z)$  is to be preferred for our detailed analysis. Since the former region has in general a higher S/N ratio we conclude that the most representative, unobscured light profiles suitable for a further study of disc truncations are obtained by vertically collapsing the surface brightness distribution between 1 and  $2h_z$  on the least obscured side of the galactic plane. (Even though this galaxy does not have a prominent dust lane nor a very large amount of patchy extinction throughout its disc,

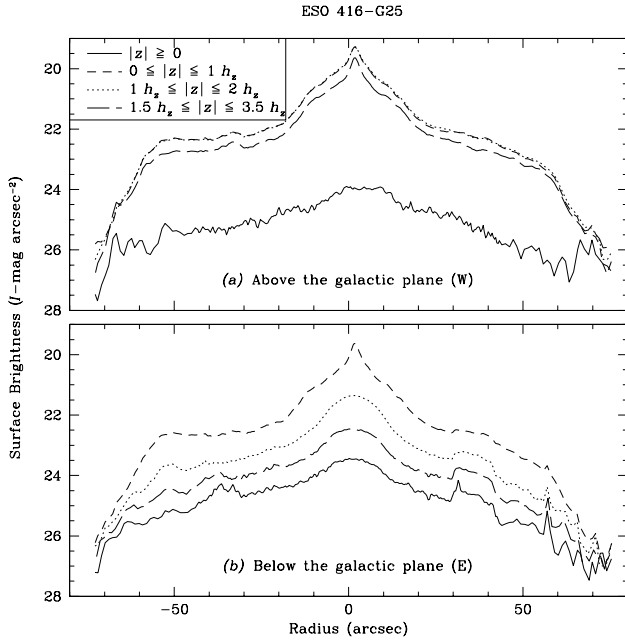


**Figure 3.** Vertically averaged radial surface brightness profiles of ESO 416-G25, taken at various  $z$ -heights from the galactic plane. To retain an approximately constant S/N ratio, a semi-logarithmic intensity-weighted radial binning algorithm has been applied to the individual profiles. An indication of the observational uncertainties is given by the background noise dominating the individual profiles at large radii.

Fig. 3 clearly shows the rationale behind choosing the least obscured side of the galactic disc [top panel].)

In the radial direction, we apply a semi-logarithmic binning algorithm, in order to retain an approximately constant overall S/N ratio (cf. de Grijs et al. 1997, de Grijs 1998), where the binning at the outermost disc radii never exceeds 2 resolution elements.

In the following sections, we will use profiles thus obtained for the detailed analysis of the truncated discs in our pilot sample.

A potential problem of this method is that the S/N ratios in the outer disc regions are often significantly lower at some (vertical) distance from the galactic planes compared to those in the planes. From Fig. 3 (and similar figures for the other sample galaxies) we conclude, however, that although the radial extent of the cut-off region appears to be a (weak) function of the height from the planes, the actual radii at which the luminosity profiles disappear asymptotically into the background noise converge to the same value of  $R_{\max}$ , within the observational uncertainties.

Secondly, some evidence exists that galactic discs thicken with increasing galactocentric distance (e.g., KS1, Kent, Dame & Fazio 1991, Barnaby & Thronson 1992, de Grijs & van der Kruit 1996, de Grijs & Peletier 1997). The signature of such a thickening of the discs on light profiles extracted parallel to the galaxies' major axes is either a flattening of the radial surface brightness profiles (if the thickening occurs gradually; e.g., Kent et al. 1991, Barnaby & Thronson 1992, de Grijs & Peletier 1997) or a locally enhanced surface brightness level at these large galactocentric

distances (if only the outermost profiles are affected; e.g., KS1, de Grijs & van der Kruit 1996). However, de Grijs & Peletier (1997) have shown that the effects of disc thickening are largest for the earliest-type spiral galaxies and almost zero for the later types, *including those examined in detail in this paper*. Moreover, even though the discs of our sample galaxies may have larger scaleheights with increasing radii, the low S/N ratios and deviations from exponentially decreasing light distributions due to, e.g., spiral arms will likely hide such observational signatures. Finally, the possible thickening of galactic discs will *not* affect the determination of the actual truncation *radius*  $R_{\max}$ , since the *radial* surface brightness distribution remains unaffected.

Although line-of-sight projection affects the observed functional form of the radial luminosity distribution, we will use a version of Eq. (2) with an exponentially decreasing functionality in the truncation region, but not including line-of-sight projection effects to fit the *truncation regions* of our sample galaxies. We chose to do so, because (i) Eq. (2) is a mathematically convenient function, and (ii) the actual profile shapes in the truncation region are erratic due to low S/N ratios and therefore the assumption of any more complicated functionality than an exponentially decreasing luminosity density cannot be taken seriously. We will perform the actual fits to our sky-subtracted images *in the linear regime* (i.e., in luminosity instead of surface brightness space), to avoid undefined surface brightness values due to “negative” noise peaks.

### 3.2 Artificial truncations?

In interpreting the steep luminosity decline as truly representative of a decrease in either the light or density distributions of a galactic disc, one has to make sure that the observed cut-off is not an artifact due to inaccurate sky subtraction. De Vaucouleurs (1948), de Vaucouleurs & Capaccioli (1979), and van Dokkum et al. (1994) have shown that inaccurate sky subtraction (i.e., oversubtraction) causes a false cut-off in the luminosity distribution of a galactic disc. This can easily be checked, because the artificial cut-off would not only be present in a major axis cut, but also in cuts taken in other directions.

In all cases, the background emission in the field of view of our sample galaxies could be well represented by a plane, of which the slope was determined by the flux in regions sufficiently far away from the galaxies in order not to be affected by residual galactic light. For most of our observations, these planes could be closely approximated by constant flux levels across the CCD field. The remaining uncertainties in the background are largely due to poisson noise.

Fig. 4 illustrates the quality of the background subtraction in the  $I$  band, where the background contribution is greater than in our other optical passbands. The left-hand panels show the minor-axis (vertical) surface brightness profiles of all sample galaxies (solid lines), radially averaged over  $\sim 20''$  in order to be able to reach similar or fainter light levels as for the profiles along the major axes, shown in the right-hand panels. We determined the sky noise,  $\sigma$ , in the regions used for the background subtraction and created new images by subtracting (background  $-2\sigma$ ), (background  $-1\sigma$ ), (background  $+1\sigma$ ), and (background  $+2\sigma$ ), where “background” represents our best estimate of the sky

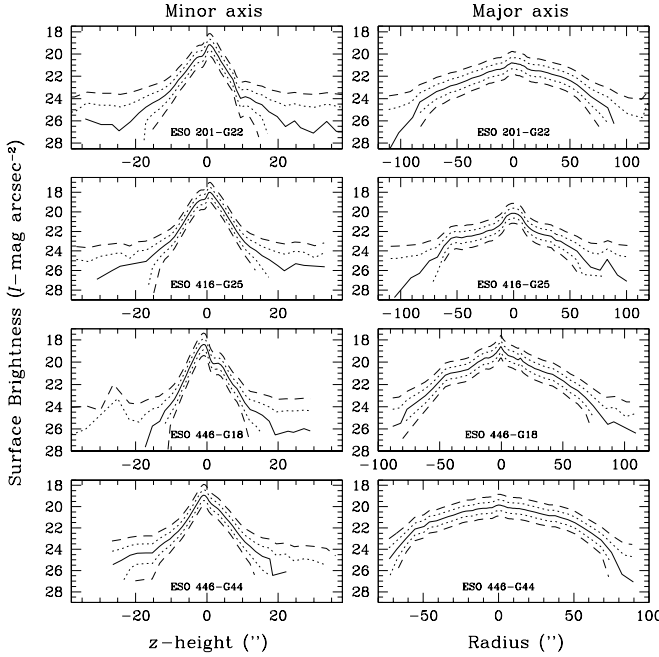


**Figure 4.** Minor-axis (left-hand panels) and major-axis (right-hand panels)  $I$ -band luminosity profiles of our sample galaxies. From top to bottom, the lines in each panel represent the minor axis profiles  $-2\sigma$  (dashed),  $-1\sigma$  (dotted), the profiles after subtraction of our best estimates for the sky background,  $+1\sigma$  (dotted lines), and  $+2\sigma$  (dashed lines), where  $\sigma$  corresponds to the sky noise in the regions that were used to determine the sky background levels. For reasons of clarity, the dashed and dotted profiles are displaced by, respectively,  $\pm 1.0$  and  $\pm 0.5$  mag from the solid lines.

background in the individual images. The under and over-subtracted profiles are shown offset from the solid profiles for reasons of clarity.

The effects of oversubtraction can clearly be seen in the minor-axis surface brightness profiles: they show artificial cut-offs and the negative background values result in undefined surface brightnesses at these  $z$  heights, above or below  $\approx 15''$  (i.e. the profiles could not be plotted beyond  $\approx 15''$  due to undefined surface brightness values resulting from oversubtraction of the sky background). Although the effects of oversubtraction on the major-axis profiles (right-hand panels; vertically averaged between  $-1.0$  and  $1.0 h_z$ ) show similar false cut-offs as for the minor-axis profiles, it appears that most of the features seen in the light profiles represented by the solid lines are real, since they are also observed in the *under*subtracted light profiles. Moreover, a qualitative comparison of both the major and the minor-axis profiles (solid lines) shows that the apparent truncations in or steepening of the major-axis light profiles do not correspond to similar cut-offs at the same surface brightness levels in the minor-axis profiles in any of our sample galaxies. We thus conclude that these features are not due to inaccurate sky subtractions, but represent real deviations from the radial exponential light profiles.

Alternatively, the detection of radially truncated discs can be artificially enhanced if the discs are strongly warped. In fact, it appears that for a number of our sample galaxies

the locus of maximum intensity at large radii may slightly deviate from the main galactic plane direction (de Grijs 1997). However, this effect is negligible for the determination of their radial truncations, because the deviations are *almost insignificant* and we average the radial luminosity profiles over a sufficiently large vertical range to avoid such problems.

In addition, effects due to the galaxies' positions near the CCD edge or to scattered light from foreground stars are potentially serious. For our four sample galaxies, the former are non-existent. As one can see in Fig. 1, both ESO 201-G22 and ESO 446-G18 suffer from the superposition of foreground stars, but only in the case of ESO 446-G18 this precludes us from determining its maximum disc radius on the northern end; the superposed foreground star near the eastern edge of ESO 201-G22 is located sufficiently far away from the truncation region, and is found on the most obscured side of the galactic plane.

### 3.3 Properties of truncated discs

#### 3.3.1 Where do the truncations occur?

In Fig. 5 we show the radial surface brightness profiles parallel to the major axis of our sample galaxies in all passbands and out to either the edge of the CCD frames or to those radii where the background noise dominates. The dashed lines indicate infinite exponential model discs, using the scale parameters obtained in Sect. 2.3. It is immediately clear that the observed surface brightness profiles are significantly fainter in the outer regions than the model discs for all galaxies in our sample and for all passbands. (Note that since these profiles are only meant to guide the eye, we have not computed the full line-of-sight integrated model profiles, although such models were, in fact, used to obtain the actual scale parameters.)

The values for both  $R_{\max}$  and  $\delta$ , resulting from the fitting of our modified version of Eq. (2) to the observed profiles using a standard linear least-squares fitting technique, are listed in Table 3. Although the formal measurement errors in  $R_{\max}$  are  $\leq 2''$ , the relatively large uncertainties associated with  $R_{\max}$  are due to the fact that  $S/N < 1$  at the truncation radius (by definition), and to the difficulty in the unambiguous determination of the start of the truncation region. In fact, the uncertainties in the truncation lengths are *predominantly* determined by the nature of  $R_{\max}$  as lower limit.

However, this method will at least produce objective estimates of  $R_{\max}$ , as opposed to visually extrapolating the observed surface brightness profiles to those radii where they would (supposedly) disappear asymptotically into the noise, as has been done previously by other workers in this field.

For a comparison with previously published results for other galaxies, we have also included the estimated truncation radii in units of the galaxies'  $I$ -band scalelengths. We chose to use the  $I$ -band scalelengths to determine the  $R_{\max}/h_R$  ratios, because these represent our longest-wavelength observations, which most likely best approximate the dominant stellar luminosity (and presumably mass) distributions (de Grijs et al. 1997, de Grijs 1998). The corresponding errors reflect the uncertainties in the determinations of both the scalelengths and the truncation radii.

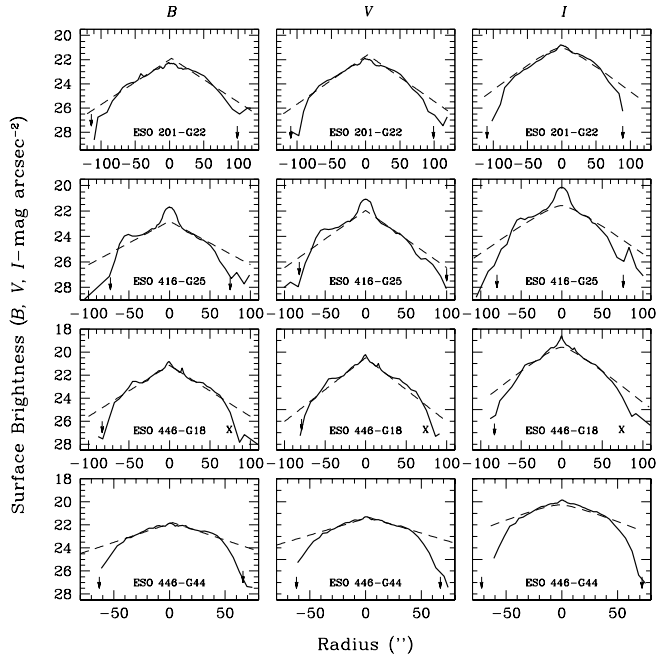


**Figure 5.** Radial surface brightness profiles of our sample galaxies taken parallel to their major axes (Sect. 3.1). Overplotted are the model exponential profiles (dashed lines), based on our full surface brightness modelling. The arrows indicate the measured truncation radii; for ESO 446-G18 the crosses indicate the side where we cannot determine the maximum radius due to the presence of foreground stars.

Van der Kruit & Searle (KS3) determined, for their small sample of large edge-ons, that the mean truncation radius  $R_{\max} \simeq (4.2 \pm 0.6)h_R$  (cf. Bottema 1995 for NGC 4013:  $R_{\max} \simeq 4.1h_R$ ). Barteldrees & Dettmar (1994) found, for a sample of 27 edge-on galaxies, a mean truncation radius of  $\simeq (3.7 \pm 1.0)h_R$ . However, this result is based on a different definition of  $R_{\max}$ : they interpreted the truncation radius as the galactocentric distance at which the observed projected radial profiles start to deviate significantly from the model exponential profiles. If we keep in mind that the truncation occurs over a finite region, then the discrepancy between these determinations can be understood. A direct comparison is therefore impossible.

Recently, Pohlen et al. (2000a) largely reanalysed Barteldrees & Dettmar's (1994) sample, assuming infinitely sharply truncated galactic discs following KS3. For their sample of 31 nearby edge-on spiral galaxies, they found  $R_{\max}/h_R = 2.9 \pm 0.7$ , significantly lower than the ratio found by KS3. This may reflect a selection bias towards large galaxies and/or small-number statistics in the KS3 sample.

While the discs of ESO 201-G22, ESO 416-G25, and ESO 446-G18 are truncated at comparable radii as found by KS and Bottema (1995), expressed in units of their disc scalelengths, ESO 446-G44 is clearly truncated at much smaller radii. This is the sample galaxy with the greatest scalelength and the only one without a bulge. ESO 446-G44, as well as ESO 416-G25, exhibit truncated discs well within the range found by Pohlen et al. (2000a).

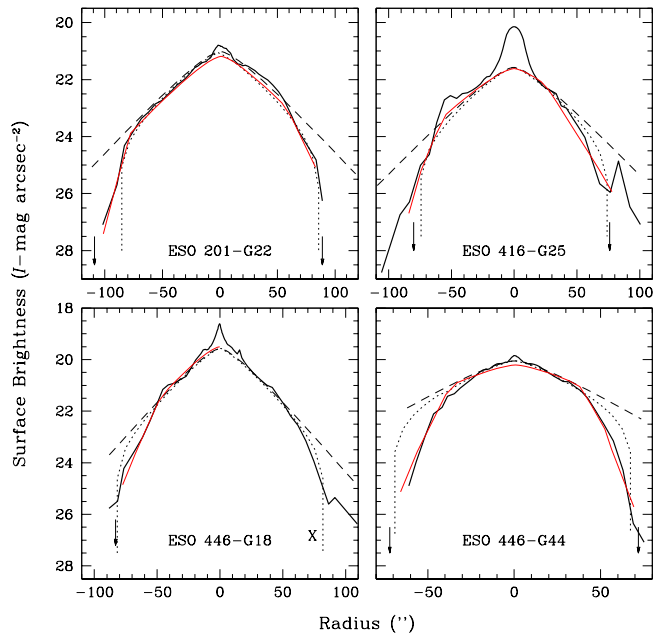


**Figure 6.** *I*-band radial surface brightness profiles of our sample galaxies taken parallel to their major axes, as in Fig. 5. Overplotted are the model exponential profiles (dashed lines), based on our full surface brightness modelling. The arrows indicate the measured truncation radii; for ESO 446-G18 the cross indicates the side where we cannot determine the maximum radius due to the presence of foreground stars. The dotted lines correspond to *infinitely sharply truncated* models, used for a comparison with previous work (Sect. 3.3.2); the thin solid lines are our model fits using a slightly modified Casertano model (Sect. 2.2).

### 3.3.2 Asymmetry and sharpness

Disc truncations do not necessarily occur at the same galactocentric distances or with the same abruptness on either side (e.g., KS1, Jensen & Thuan 1982, Näslund & Jörsäter 1997, Abe et al. 1999, Fry et al. 1999). In most cases, however, the truncation radii on either side of the galactic disc occur within  $\sim 10 - 15\%$  of each other. The profiles in Figs. 5 and 6, and our estimates for  $R_{\max}$  in Table 3 show that in general, the discs of our sample galaxies are truncated at similar radii, within their observational uncertainties, with the possible exception of ESO 201-G22.

Table 3 also contains our best estimates for the exponential scalelength in the truncation region,  $h_{R,\delta}$ . To measure this scalelength, we defined the inner fitting radius as the radius where the radial surface brightness profile starts to deviate significantly from the model radial exponential light distribution (cf. Barteldrees & Dettmar 1994); the uncertainty in this radius is generally  $\leq 15\%$ , depending on the particular galaxy considered. As outer fitting boundary we used  $R_{\max}$ . The errors associated with  $h_{R,\delta}$  are observational uncertainties, obtained from the comparison of several similar fits in which we adjusted the inner boundary of the radial fitting range by 10–20%. The uncertainties in  $R_{\max}$  are included in the observational errors given; the formal errors were  $\leq 1\%$ . The effects on disc truncations and scale parameters of an inclination  $i \neq 90^\circ$  are negligible for our

**Table 3.** Disc truncations in our sample galaxies

Columns: (1) Galaxy name; (2) Passband observed in; (3) Side of the galactic centre; (4) and (5) Cut-off radius (lower limit) and observational error (arcsec); (6) and (7) Cut-off radius (in units of the  $I$ -band scalelength) and observational error; (8) Truncation length (arcsec; typical observational uncertainties are of order  $\geq 10''$ ); (9) and (10) Scalelength in the truncation region and observational error, in arcsec; (11) and (12) Scalelength in the truncation region and observational error, in kpc (based on the heliocentric velocities obtained by Mathewson, Ford & Buchhorn 1992 [see de Grijs 1998])

Galaxy (ESO-LV)	Band (1)	Side (2)	$R_{\max}$ ( $''$ ) (3)	$\pm$ (4) (5)	$R_{\max}$ ( $h_{R,I}$ ) (6)	$\pm$ (7) (8)	$\delta$ ( $''$ ) (9)	$h_{R,\delta}$ ( $''$ ) (10)	$\pm$ (11) (12)	$h_{R,\delta}$ ( $h^{-1}$ kpc) (11)	
201-G22	<i>B</i>	E	114	10	4.9	0.4	44	14.2	1.0	3.0	
		W	99	4	4.2	0.2	50	16.8	0.9	3.6	
		<i>V</i>	109	3	4.7	0.1	26	16.4	0.3	3.5	
		W	99	10	4.2	0.4	50	15.7	0.4	3.4	
		<i>I</i>	109	10	4.7	0.4	28	17.6	0.3	3.8	
	<i>I</i>	W	89	8	3.8	0.3	31	12.9	0.2	2.8	
		<i>B</i>	N	73	5	3.3	0.2	13	6.2	1.6	
		S	75	10	3.3	0.5	30	10.6	1.4	2.9	
		<i>V</i>	N	82	10	3.7	0.5	24	7.2	1.0	
		S	100	15	4.5	0.7	60	14.9	0.3	4.1	
416-G25	<i>I</i>	N	80	15	3.6	0.7	28	9.2	1.7	2.6	
		S	76	10	3.4	0.5	53	14.3	1.3	4.0	
	<i>B</i>	S	83	8	4.6	0.4	35	11.6	0.6	2.8	
		<i>V</i>	S	79	8	4.4	0.4	31	10.3	0.3	2.5
446-G18	<i>I</i>	S	83	8	4.6	0.4	35	9.8	1.0	2.4	
	<i>B</i>	E	66	8	2.3	0.3	25	10.2	0.2	1.6	
		W	63	8	2.1	0.3	22	7.6	0.8	1.2	
		<i>V</i>	E	67	8	2.3	0.3	27	8.6	1.3	1.3
		W	62	8	2.1	0.3	22	7.6	0.8	1.2	
	<i>I</i>	E	72	7	2.4	0.3	33	9.8	0.3	1.5	
		W	72	8	2.4	0.3	32	8.6	0.3	1.3	
										0.1	

galaxy sample of  $i \geq 87^\circ$  inclined galaxies, as was convincingly shown by Barteldrees & Dettmar (1994), in particular in view of the systematic and observational uncertainties involved. The combination of  $h_{R,\delta}$  and  $\delta$  gives us an indication of the asymmetry and sharpness of the actual disc truncations.

Considering the relatively large systematic and observational errors that cannot be avoided at this point, we cannot claim that we detect any systematic asymmetries, perhaps with the exception of ESO 416-G25. The northern edge of the disc of ESO 416-G25 is very sharply truncated compared to its southern edge. Upon close examination of the actual CCD images, we believe that this may be explained by the fact that we likely observe the outer stellar envelope of a spiral arm, whereas on the southern side we are looking into the inside of a spiral arm. Note, however, that also at the southern edge of the disc a clear truncation signature is observed (Fig. 5).

The last two columns of Table 3 show that in none of our sample galaxies the radial scalelength in the truncation region decreases to values of order or less than 1 kpc. Using  $H_0 = 50 \text{ km s}^{-1} \text{ Mpc}^{-1}$ , or other values closer to the current best estimate, will further increase the truncation scalelengths measured in our galaxies. Although two of our sample galaxies may not be exactly edge-on, their inclinations are sufficiently close to  $90^\circ$  so as not to increase the measurements of  $h_{R,\delta}$  by more than their observational uncertainties (cf. Barteldrees & Dettmar 1994). We are therefore forced to conclude that, although our discs are clearly

truncated, the truncation occurs over a larger region and not as abruptly as found in previous studies.

As a comparison between our approach and that used in previous work, in Fig. 6 we present enlarged versions of the  $I$ -band profiles of Fig. 5, in which we show both our best-fit radial profiles using a slightly modified Casertano model (Sect. 2.2; thin solid lines) and the corresponding profiles for a symmetric, projected, sharply truncated exponential disc, with the disc truncations occurring at  $R_{\max}$  (dotted lines). These profiles were obtained by applying the same method used to extract the observed profiles used for Fig. 5 to model images of our sample galaxies. From a comparison between these dotted lines and the actual, observed profiles, it is clear that the discs of our sample galaxies are generally *not infinitely sharply truncated*, but show a more gradual decrease of their radial luminosity density.

Finally, from a galaxy-by-galaxy inspection of the values for  $R_{\max}$ , no apparent trend with wavelength can be discerned, within the observational errors. However, a detailed comparison of the radial  $(B - I)$  colour profiles, our longest colour baseline, reveals that the disc colour tends to get bluer in the truncation region compared to the colours in the main disc (Fig. 7). A similar result was obtained by Sasaki (1987) for the truncation region of NGC 5907. Although this may be indicative of more recent star formation at the edge of the discs (e.g., Larson 1976, Seiden et al. 1984), the opposite behaviour is exhibited both on the northern side of the disc of ESO 416-G25, and on the western side of the disc of ESO 446-G44, where the colour reddens in the truncation region. This is confirmed by the fact that at these edges,

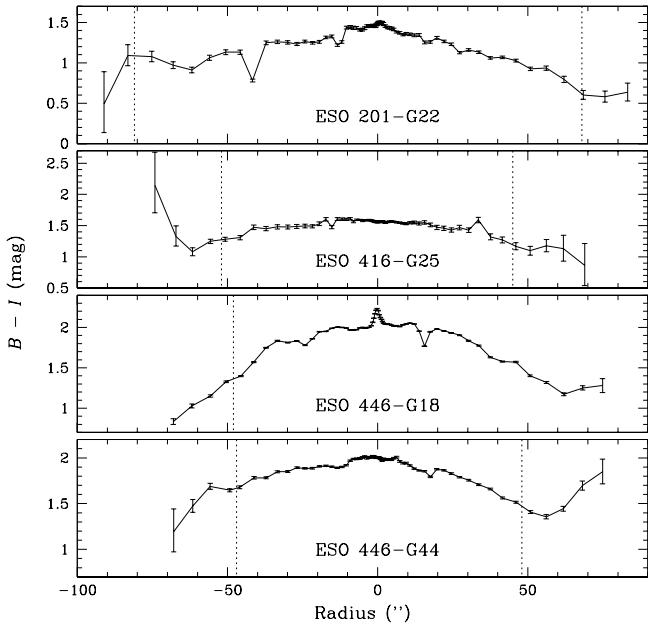


**Figure 7.** Radial ( $B - I$ ) colour profiles of our sample galaxies parallel to their major axes, constructed from the profiles shown in Fig. 5. The dashed lines indicate the approximate start of the truncation regions. All data points with colour uncertainties  $\sigma_{(B-I)} \leq 0.4$  mag have been included.

these discs appear to be more sharply truncated in the  $B$  band compared to the  $I$ -band observations, which may be the signature of a spiral arm.

#### 4 DYNAMICAL CONSEQUENCES OF DISC TRUNCATIONS: OUTLOOK

Although the fact that many spiral discs seem to have truncated stellar discs is an interesting observation in the context of galactic structure, the physical implications of a similar truncation in the mass distribution of galactic discs has far-reaching consequences making the study of disc truncations fundamental to our understanding of galactic disc maintenance and evolution. This is therefore the main science driver of our attempts to define a unique and objective method to measure disc truncations.

##### 4.1 Edge smearing and disc asymmetries

The persistence of sharp disc cut-offs places a strong upper limit on the stellar velocity dispersion at the disc edge (KS1). Adopting a rotational velocity of  $250 \text{ km s}^{-1}$  at  $20 \text{ kpc}$  for NGC 4565, the radial stellar velocity dispersion,  $\langle v_R^2 \rangle^{1/2}$ , must be  $\leq 10 \text{ km s}^{-1}$  so that random motions do not wash out the sharp cut-off within one revolution time (Jensen & Thuan 1982; see also KS1, May & James 1984), or the sharp cut-off must be a transient feature (e.g., Sasaki 1987). This low upper limit for  $\langle v_R^2 \rangle^{1/2}$  is close to the minimum value of  $\sim 2 \text{ km s}^{-1}$  needed to satisfy Toomre's (1964) criterion of local stability for disc galaxies, and thus for star formation.

Alternatively, in the case of a disc formation scenario in

which the disc grows from the inside outward (e.g., Larson 1976, Gunn 1982, Seiden 1983, Seiden et al. 1984) a sharp edge can be maintained if this outward growth is sufficiently rapid, so that the random motion of the stars does not smear out the edge. Note, however, that the disc truncations in our sample galaxies are not as sharp as those found by KS1–4, among others, which will relax these requirements.

The situation becomes more complicated if the galactic disc is lopsided or if the truncations occur at different radii. Following the epicyclic description of Baldwin, Lynden-Bell & Sancisi (1980), van der Kruit (1988) estimates a smearing time of  $1.7 \times 10^{10} \text{ yr}$  for the Galactic disc, and he concludes that a variation in the truncation radii of order 10% may just survive a Hubble time. With the possible exception of ESO 416-G25, our sample galaxies appear to comfortably meet this requirement.

##### 4.2 Rotation curves as diagnostic tools

Casertano (1983) has shown that a truncated stellar disc leaves a signature on the rotation curve in the form of a region of slowly varying velocity followed by a steep decline just outside the truncation radius (see also Hunter, Ball & Gottesman 1984). The amount of this decrease is a measure of the disc mass. The effect of a truncation is a *flattening* of the rotation curve inside the truncation itself, from some radius  $R_0$  to  $R_{\max}$ , and a steep decrease of the velocity outside.

The well-known warped edge-on galaxy NGC 4013, for which Bottema (1995) suspected a sudden decrease in the mass density corresponding to the truncation radius, has indeed been shown to exhibit a sudden drop in the rotational velocity of about  $20 \text{ km s}^{-1}$  just at the optical edge (Bottema, Shostak & van der Kruit 1987, Bottema 1995, 1996). This drop can be understood if one realises that near the edge of the galactic disc the mass distribution will be irregular: there is no smooth, circular end to the disc, but it likely ends in spiral arms. Bottema (1996) argues that therefore gas moving in the potential of such patches of stellar matter will not be in precise circular motion and hence the radial velocity along the line of sight is somewhat lower than the true rotation.

Finally, Bahcall (1983) showed that, for Sb or Sc galaxies like NGC 891 or the Galaxy, the feature in the rotation curve due to the truncated stellar disc is observable only if  $R_{\max} \leq 4h_R$  (smaller for galaxies with more prominent bulges), if the truncation length is small compared to  $h_R$ , and if the halo mass inside  $R_{\max}$  is smaller than the disc mass (Casertano 1983).

Unfortunately, the currently available velocity information for the four galaxies in our pilot sample does not allow us to confirm the presence of sharp truncations in the disc mass based on the shape of the rotation curves: only for ESO 446-G18 and ESO 446-G44 rotation curves have been published, for the  $\text{H}\alpha$  emission (Mathewson et al. 1992) and the  $\text{H}\text{I}$  component (Persic & Salucci 1995, based on the raw Mathewson et al. 1992 data), but these rotation curves do not or just barely reach those radii where we expect to be able to see a truncation signature.

## 5 SUMMARY AND CONCLUSIONS

In this paper we have presented the first results of a systematic analysis of galactic disc structure in general and of radially truncated exponential discs in particular for a pilot sample of four “normal” disc-dominated edge-on spiral galaxies. We have carefully considered the importance of (residual) dust, deviations from 90° inclinations, and spiral arms, and concluded that these effects do not affect our results significantly. We have also shown that the truncated discs in our sample galaxies are not caused artificially by inaccurate sky subtraction, but are real deviations from the radial exponential light profiles.

An independent approach to obtain the statistics of truncated galactic discs, using a sample of galaxies selected in a uniform way, is needed in order to better understand their overall properties and physical implications. If the truncations seen in the stellar light are also present in the mass distribution, they would have important dynamical consequences at the disc’s outer edges. We have shown that the truncated luminosity distributions of our pilot sample galaxies, if also present in the mass distributions, comfortably meet the requirements for longevity.

The truncation radii, expressed in units of  $h_R$ , for the discs of ESO 201-G22, ESO 416-G25, and ESO 446-G18 are comparable to those found by KS1-4 and Bottema (1995), while ESO 446-G44 is truncated at much smaller radii. In fact, the truncations of the discs of ESO 416-G25 and ESO 446-G44 are within the range found by Pohlen et al. (2000a) for their sample of 31 nearby edge-on spiral galaxies. In general, the discs of our sample galaxies are truncated at similar radii on either side of their centres, within the observational uncertainties, with the exception of ESO 201-G22.

With the possible exception of the disc of ESO 416-G25, it appears that our sample galaxies are fairly symmetric, in terms of both the sharpness of their disc truncations and the truncation length, although the truncations occur over a larger region and not as abruptly as found in previous studies. The northern edge of the disc of ESO 416-G25 is very sharply truncated compared to its southern edge. We believe that this may be explained by the fact that we likely observe the outer stellar envelope of a spiral arm, whereas on the southern side we are looking into the inside of a spiral arm.

## ACKNOWLEDGMENTS

We thank Piet van der Kruit for stimulating discussions and acknowledge useful suggestions by the referee, M. Pohlen. This work is partially based on the undergraduate senior thesis of KHW at the University of Virginia. RdeG acknowledges partial funding from NASA grants NAG 5-3428 and NAG 5-6403 and hospitality at the University of Groningen. This research has made use of NASA’s Astrophysics Data System Abstract Service and of the NASA/IPAC Extragalactic Database (NED).

## REFERENCES

Abe F., Bond I.A., Carter B.S., et al., 1999, AJ, 118, 261  
 Bahcall J.N., 1983, ApJ, 267, 52

Baldwin J.E., Lynden-Bell D., Sancisi R., 1980, MNRAS, 193, 313  
 Barnaby D., Thronson Jr. H.A., 1992, AJ, 103, 41  
 Barteldrees A., Dettmar R.-J., 1994, A&AS, 103, 475  
 Bottema R., 1995, A&A, 295, 605  
 Bottema R., 1996, A&A, 306, 345  
 Bottema R., Shostak G.S., van der Kruit P.C., 1987, Nat, 328, 401  
 Casertano S., 1983, MNRAS, 203, 735  
 de Grijs R., 1997, PhD Thesis, Univ. of Groningen, the Netherlands  
 de Grijs R., 1998, MNRAS, 299, 595  
 de Grijs R., Peletier R.F., 1997, A&A, 320, L21  
 de Grijs R., Peletier R.F., van der Kruit P.C., 1997, A&A, 327, 966  
 de Grijs R., van der Kruit P.C., 1996, A&AS, 117, 19  
 de Jong R.S., 1995, PhD Thesis, Univ. of Groningen, the Netherlands  
 de Vaucouleurs G., 1948, Ann. Astrophys., 11, 247  
 de Vaucouleurs G., Capaccioli M., 1979, ApJS, 40, 699  
 Freeman K.C., 1970, ApJ, 160, 811  
 Fry A.M., Morrison H.L., Harding P., Borošon T.A., 1999, AJ 118, 1209  
 Giovanelli R., Haynes M.P., Salzer J.J., Wegner G., Da Costa L.N., Freudling W., 1994, AJ, 107, 2036  
 Gunn J.E., 1982, in: Astrophysical cosmology, Proceedings of the Study Week on Cosmology and Fundamental Physics, Vatican City State, p. 233  
 Hunter Jr. J.H., Ball R., Gottesman S.T., 1984, MNRAS, 208, 1  
 Jensen E.B., Thuan T.X., 1982, ApJS, 50, 421  
 Kent S.M., Dame T.M., Fazio G., 1991, ApJ, 378, 131  
 Knapen J.H., van der Kruit P.C., 1991, A&A, 248, 57  
 Kregel M., van der Kruit P.C., de Grijs R., 2001, MNRAS, submitted  
 Kylafis N.D., Bahcall J.N., 1987, ApJ, 317, 637  
 Larson R.B., 1976, MNRAS, 176, 31  
 Lauberts A., Valentijn E.A., 1989, The Surface Photometry Catalogue of the ESO-Uppsala Galaxies, Garching bei München: ESO (ESO-LV)  
 Lequeux J., Dantel-Fort M., Fort B., 1995, A&A, 296, L13  
 Mathewson D.S., Ford V.L., Buchhorn M., 1992, ApJS, 81, 413  
 May A., James R.A., 1984, MNRAS, 206, 691  
 Morrison H.L., Borošon T.A., Harding P., 1994, AJ, 108, 1191  
 Näslund M., Jörsäter S., 1997, A&A, 325, 915  
 Persic M., Salucci P., 1995, ApJS, 99, 501  
 Pohlen M., Dettmar R.-J., Lüticke R., 2000a, A&A, 357, L1  
 Pohlen M., Dettmar R.-J., Lüticke R., Schwarzkopf U., 2000b, A&AS, 144, 405  
 Sasaki T., 1987, PASJ, 39, 849  
 Seiden P.E., 1983, ApJ, 266, 555  
 Seiden P.E., Schulman L.S., Elmegreen B.G., 1984, ApJ, 282, 95  
 Shaw M.A., Gilmore G., 1990, MNRAS, 242, 59  
 Toomre A., 1964, ApJ, 139, 1217  
 van der Kruit P.C., 1988, A&A, 192, 117  
 van der Kruit P.C., Searle L., 1981a, A&A, 95, 105 (KS1)  
 van der Kruit P.C., Searle L., 1981b, A&A, 95, 116 (KS2)  
 van der Kruit P.C., Searle L., 1981a, A&A, 110, 61 (KS3)  
 van der Kruit P.C., Searle L., 1981b, A&A, 110, 79 (KS4)  
 van Dokkum P.G., Peletier R.F., de Grijs R., Balcells M., 1994, A&A, 286, 415  
 Xilouris E.M., Kylafis N.D., Papamastorakis J., Paleologou E.V., Haerendel G., 1997, A&A, 325, 135